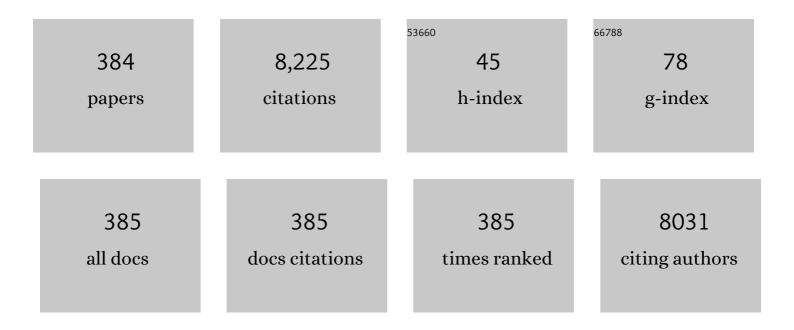
List of Publications by Year in descending order

Source: https://exaly.com/author-pdf/1147687/publications.pdf Version: 2024-02-01



LUN CHEN

#	Article	IF	CITATIONS
1	Large-Area Nanowire Arrays of Molybdenum and Molybdenum Oxides: Synthesis and Field Emission Properties. Advanced Materials, 2003, 15, 1835-1840.	11.1	347
2	Needle-shaped silicon carbide nanowires: Synthesis and field electron emission properties. Applied Physics Letters, 2002, 80, 3829-3831.	1.5	245
3	Room-Temperature Strong Light–Matter Interaction with Active Control in Single Plasmonic Nanorod Coupled with Two-Dimensional Atomic Crystals. Nano Letters, 2017, 17, 4689-4697.	4.5	237
4	Growth and field-emission property of tungsten oxide nanotip arrays. Applied Physics Letters, 2005, 87, 223108.	1.5	219
5	Electrical and Photosensitive Characteristics of a-IGZO TFTs Related to Oxygen Vacancy. IEEE Transactions on Electron Devices, 2011, 58, 1121-1126.	1.6	217
6	Field emission from crystalline copper sulphide nanowire arrays. Applied Physics Letters, 2002, 80, 3620-3622.	1.5	191
7	Aâ€site Cation Engineering for Highly Efficient MAPbl ₃ Single rystal Xâ€ray Detector. Angewandte Chemie - International Edition, 2019, 58, 17834-17842.	7.2	174
8	Temperature dependence of field emission from cupric oxide nanobelt films. Applied Physics Letters, 2003, 83, 746-748.	1.5	165
9	Polymerized carbon nanobells and their field-emission properties. Applied Physics Letters, 1999, 75, 3105-3107.	1.5	164
10	Metal-like single crystalline boron nanotubes: synthesis and in situ study on electric transport and field emission properties. Journal of Materials Chemistry, 2010, 20, 2197.	6.7	157
11	Graphitization of nanodiamond powder annealed in argon ambient. Applied Physics Letters, 1999, 74, 3651-3653.	1.5	143
12	Correlation between Resistance and Field Emission Performance of Individual ZnO One-Dimensional Nanostructures. ACS Nano, 2008, 2, 2015-2022.	7.3	134
13	Synthesis and field-emission properties of aligned MoO3 nanowires. Applied Physics Letters, 2003, 83, 2653-2655.	1.5	131
14	Mechanism Responsible for Initiating Carbon Nanotube Vacuum Breakdown. Physical Review Letters, 2004, 93, 075501.	2.9	123
15	Lowâ€Voltage Photodetectors with High Responsivity Based on Solutionâ€Processed Micrometerâ€Scale Allâ€Inorganic Perovskite Nanoplatelets. Small, 2017, 13, 1700364.	5.2	119
16	Self-heated hydrogen gas sensors based on Pt-coated W18O49 nanowire networks with high sensitivity, good selectivity and low power consumption. Sensors and Actuators B: Chemical, 2011, 153, 354-360.	4.0	105
17	Study of Physical and Chemical Processes of H ₂ Sensing of Pt-Coated WO ₃ Nanowire Films. Journal of Physical Chemistry C, 2010, 114, 15504-15509.	1.5	100
18	Fabrication of Vertically Aligned Singleâ€Crystalline Boron Nanowire Arrays and Investigation of Their Fieldâ€Emission Behavior. Advanced Materials, 2008, 20, 2609-2615.	11.1	99

#	Article	IF	CITATIONS
19	Morphology Effect of Vertical Graphene on the High Performance of Supercapacitor Electrode. ACS Applied Materials & Interfaces, 2016, 8, 7363-7369.	4.0	98
20	Gasochromic effect and relative mechanism of WO3nanowire films. Nanotechnology, 2007, 18, 205701.	1.3	95
21	Catalyst-free synthesis of ZnO nanowire arrays on zinc substrate by low temperature thermal oxidation. Materials Letters, 2007, 61, 666-670.	1.3	93
22	Ultrathin Seed-Layer for Tuning Density of ZnO Nanowire Arrays and Their Field Emission Characteristics. Journal of Physical Chemistry C, 2008, 112, 11685-11690.	1.5	91
23	Optimize the field emission character of a vertical few-layer graphene sheet by manipulating the morphology. Nanotechnology, 2012, 23, 015202.	1.3	91
24	Large-Scale Synthesis of Bicrystalline ZnO Nanowire Arrays by Thermal Oxidation of Zinc Film: Growth Mechanism and High-Performance Field Emission. Crystal Growth and Design, 2013, 13, 2897-2905.	1.4	90
25	Field emission study of SiC nanowires/nanorods directly grown on SiC ceramic substrate. Applied Physics Letters, 2006, 89, 023118.	1.5	85
26	Vacuum gap dependence of field electron emission properties of large area multi-walled carbon nanotube films. Journal Physics D: Applied Physics, 2001, 34, 1597-1601.	1.3	72
27	Segregation Behaviors and Radial Distribution of Dopant Atoms in Silicon Nanowires. Nano Letters, 2011, 11, 651-656.	4.5	72
28	Catalytic synthesis and photoluminescence of needle-shaped 3C–SiC nanowires. Solid State Communications, 2003, 128, 295-297.	0.9	71
29	Transmission type flat-panel X-ray source using ZnO nanowire field emitters. Applied Physics Letters, 2015, 107, .	1.5	71
30	Physical origin of nonlinearity in the Fowler–Nordheim plot of field-induced emission from amorphous diamond films: Thermionic emission to field emission. Applied Physics Letters, 2000, 76, 2463-2465.	1.5	69
31	Vacuum breakdown of carbon-nanotube field emitters on a silicon tip. Applied Physics Letters, 2003, 83, 2671-2673.	1.5	66
32	Controllable preparation of 1-D and dendritic ZnO nanowires and their large area field-emission properties. Journal of Alloys and Compounds, 2017, 690, 304-314.	2.8	66
33	A Catalyzed-Growth Route to Directly Form Micropatterned WO ₂ and WO ₃ Nanowire Arrays with Excellent Field Emission Behaviors at Low Temperature. Crystal Growth and Design, 2010, 10, 5193-5199.	1.4	64
34	Optimizing the Field Emission Properties of ZnO Nanowire Arrays by Precisely Tuning the Population Density and Application in Large-Area Gated Field Emitter Arrays. ACS Applied Materials & Interfaces, 2017, 9, 3911-3921.	4.0	64
35	Synthesis of silicon carbide nanowires in a catalyst-assisted process. Chemical Physics Letters, 2002, 356, 511-514.	1.2	61
36	Field emission display device structure based on double-gate driving principle for achieving high brightness using a variety of field emission nanoemitters. Applied Physics Letters, 2007, 90, 253105.	1.5	61

#	Article	IF	CITATIONS
37	Synthesis of crystalline alumina nanowires and nanotrees. Chemical Physics Letters, 2002, 365, 505-508.	1.2	60
38	Fabrication of vertically aligned Si nanowires and their application in a gated field emission device. Applied Physics Letters, 2006, 88, 013112.	1.5	60
39	Excitation Wavelength Dependent Luminescence of LuNbO ₄ :Pr ³⁺ —Influences of Intervalence Charge Transfer and Host Sensitization. Journal of Physical Chemistry C, 2016, 120, 26044-26053.	1.5	60
40	Resonance Coupling in Silicon Nanosphere–J-Aggregate Heterostructures. Nano Letters, 2016, 16, 6886-6895.	4.5	58
41	Tailoring of electromagnetic field localizations by two-dimensional graphene nanostructures. Light: Science and Applications, 2017, 6, e17057-e17057.	7.7	56
42	Yellow-emitting NaCaPO_4:Mn^2+ phosphor for field emission displays. Optics Express, 2011, 19, 16423.	1.7	53
43	A Fully-Sealed Carbon-Nanotube Cold-Cathode Terahertz Gyrotron. Scientific Reports, 2016, 6, 32936.	1.6	53
44	Host-sensitized luminescence of Dy ³⁺ in LuNbO ₄ under ultraviolet light and low-voltage electron beam excitation: energy transfer and white emission. Journal of Materials Chemistry C, 2017, 5, 9012-9020.	2.7	53
45	Enhanced Detectivity and Suppressed Dark Current of Perovskite–InGaZnO Phototransistor via a PCBM Interlayer. ACS Applied Materials & Interfaces, 2018, 10, 44144-44151.	4.0	50
46	Growth of Large-Area Aligned Molybdenum Nanowires by High Temperature Chemical Vapor Deposition:Â Synthesis, Growth Mechanism, and Device Application. Journal of Physical Chemistry B, 2006, 110, 10296-10302.	1.2	47
47	Ultrafast Fieldâ€Emission Electron Sources Based on Nanomaterials. Advanced Materials, 2019, 31, e1805845.	11.1	46
48	Fabrication of Ru and Ru-Based Functionalized Nanotubes. Journal of the American Chemical Society, 2004, 126, 3060-3061.	6.6	45
49	Effects of light illumination on field emission from CuO nanobelt arrays. Applied Physics Letters, 2005, 86, 151107.	1.5	44
50	Enhancing electron emission from silicon tip arrays by using thin amorphous diamond coating. Applied Physics Letters, 1998, 73, 3668-3670.	1.5	43
51	An approach for synthesizing various types of tungsten oxide nanostructure. Nanotechnology, 2006, 17, 5590-5595.	1.3	43
52	Physical origin of non-linearity in Fowler–Nordheim plots of aligned large area multi-walled nitrogen-containing carbon nanotubes. Materials Science & Engineering A: Structural Materials: Properties, Microstructure and Processing, 2002, 327, 16-19.	2.6	42
53	Cathodoluminescent properties of nanocrystalline Lu3Ga5O12:Tb3+ phosphor for field emission display application. Journal of Vacuum Science and Technology B:Nanotechnology and Microelectronics, 2010, 28, 490-494.	0.6	42
54	Site Occupation of Eu ²⁺ in Ba _{2–<i>x</i>} Sr _{<i>x</i>} SiO ₄ (<i>x</i> = 0–1.9) and Origin of Improved Luminescence Thermal Stability in the Intermediate Composition. Inorganic Chemistry, 2018, 57, 7090-7096.	1.9	42

#	Article	IF	CITATIONS
55	Synthesis of large-scaled MoO2 nanowire arrays. Chemical Physics Letters, 2003, 382, 443-446.	1.2	40
56	On achieving better uniform carbon nanotube field emission by electrical treatment and the underlying mechanism. Applied Physics Letters, 2006, 88, 111501.	1.5	40
57	Effect of structural parameter on field emission properties of semiconducting copper sulphide nanowire films. Journal of Applied Physics, 2003, 93, 1774-1777.	1.1	39
58	Fabrication of large-area ZnO nanowire field emitter arrays by thermal oxidation for high-current application. Applied Surface Science, 2019, 484, 966-974.	3.1	37
59	Large-area aligned branched Cu ₂ S nanostructure arrays: room-temperature synthesis and growth mechanism. Nanotechnology, 2010, 21, 215602.	1.3	36
60	Ultrafast optical emission of nanodiamond induced by laser excitation. Applied Physics Letters, 2004, 85, 914-916.	1.5	35
61	Nanomaterials for field electron emission: preparation, characterization and application. Ultramicroscopy, 2003, 95, 19-28.	0.8	34
62	Fully sealed carbon nanotube flat-panel light source and its application as thin film transistor–liquid-crystal display backlight. Journal of Vacuum Science & Technology B, 2008, 26, 1033-1037.	1.3	34
63	High luminescent Li_2CaSiO_4:Eu^2+ cyan phosphor film for wide color gamut field emission display. Optics Express, 2012, 20, 17701.	1.7	34
64	A double-sided radiating flat-panel X-ray source using ZnO nanowire field emitters. Vacuum, 2017, 144, 266-271.	1.6	34
65	Electron Bombardment Induced Photoconductivity and High Gain in a Flat Panel Photodetector Based on a ZnS Photoconductor and ZnO Nanowire Field Emitters. ACS Photonics, 2018, 5, 4147-4155.	3.2	34
66	Inorganic Boron-Based Nanostructures: Synthesis, Optoelectronic Properties, and Prospective Applications. Nanomaterials, 2019, 9, 538.	1.9	34
67	Electrochromic properties of WO3 nanowire films and mechanism responsible for the near infrared absorption. Journal of Applied Physics, 2007, 101, 114303.	1.1	33
68	Investigation of the effects of atomic oxygen exposure on the electrical and field emission properties of ZnO nanowires. Applied Surface Science, 2013, 270, 82-89.	3.1	32
69	Individual Boron Nanowire Has Ultra-High Specific Young's Modulus and Fracture Strength As Revealed by <i>in Situ</i> Transmission Electron Microscopy. ACS Nano, 2013, 7, 10112-10120.	7.3	32
70	The application of carbon nanotubes in high-efficiency low power consumption field-emission luminescent tube. Ultramicroscopy, 2003, 95, 153-156.	0.8	31
71	A novel lift-off method for fabricating patterned and vertically-aligned W18O49 nanowire arrays with good field emission performance. Nanoscale, 2011, 3, 1850.	2.8	31
72	Surface nitrogen functionality for the enhanced field emission of free-standing few-layer graphene nanowalls. Journal of Alloys and Compounds, 2016, 672, 433-439.	2.8	31

#	Article	IF	CITATIONS
73	A Flat Panel Photodetector Formed by a ZnS Photoconductor and ZnO Nanowire Field Emitters Achieving High Responsivity From Ultraviolet to Visible Light for Indirect-Conversion X-Ray Imaging. Journal of Lightwave Technology, 2018, 36, 5010-5015.	2.7	31
74	Fabrication of gated CuO nanowire field emitter arrays for application in field emission display. Journal of Vacuum Science and Technology B:Nanotechnology and Microelectronics, 2010, 28, 558-561.	0.6	29
75	A Mo nanoscrew formed by crystalline Mo grains with high conductivity and excellent field emission properties. Nanoscale, 2014, 6, 4659-4668.	2.8	29
76	Growth of Largeâ€Scale Boron Nanowire Patterns with Identical Baseâ€Up Mode and In Situ Field Emission Studies of Individual Boron Nanowire. Small, 2014, 10, 685-693.	5.2	29
77	Integration of ZnO nanowires in gated field emitter arrays for large-areaÂvacuum microelectronics applications. Current Applied Physics, 2017, 17, 85-91.	1.1	29
78	High-voltage triode flat-panel display using field-emission nanotube-based thin films. Journal of Vacuum Science & Technology an Official Journal of the American Vacuum Society B, Microelectronics Processing and Phenomena, 2001, 19, 1370.	1.6	28
79	Controlled synthesis of ultra-long AlNnanowires in different densities and in situ investigation of the physical properties of an individual AlNnanowire. Nanoscale, 2011, 3, 610-618.	2.8	27
80	Investigation on the photoconductive behaviors of an individual AIN nanowire under different excited lights. Nanoscale Research Letters, 2012, 7, 454.	3.1	27
81	Defect-Enhanced Field Emission from WO3 Nanowires for Flat-Panel X-ray Sources. ACS Applied Nano Materials, 2019, 2, 5206-5213.	2.4	27
82	Cathodoluminescent properties of SrGa[sub 2]S[sub 4]:Eu[sup 2+] phosphor for field-emission display applications. Journal of Vacuum Science & Technology B, 2007, 25, 618.	1.3	26
83	Large-scale fabrication of ordered arrays of microcontainers and the restraint effect on growth of CuO nanowires. Nanoscale Research Letters, 2011, 6, 86.	3.1	26
84	Study of field emission, electrical transport, and their correlation of individual single CuO nanowires. Journal of Applied Physics, 2011, 109, .	1.1	26
85	Thermo-enhanced field emission from ZnO nanowires: Role of defects and application in a diode flat panel X-ray source. Applied Surface Science, 2017, 399, 337-345.	3.1	26
86	Flat-panel luminescent lamp using carbon nanotube cathodes. Journal of Vacuum Science & Technology an Official Journal of the American Vacuum Society B, Microelectronics Processing and Phenomena, 2003, 21, 1727.	1.6	25
87	Silicon tip arrays with ultrathin amorphous diamond apexes. Applied Physics Letters, 2002, 81, 4257-4259.	1.5	24
88	Dual-Gate Photosensitive Thin-Film Transistor-Based Active Pixel Sensor for Indirect-Conversion X-Ray Imaging. IEEE Transactions on Electron Devices, 2015, 62, 2894-2899.	1.6	24
89	Growth direction manipulation of few-layer graphene in the vertical plane with parallel arrangement. Carbon, 2013, 56, 103-108.	5.4	23
90	εâ€Ga ₂ O ₃ Thin Film Avalanche Lowâ€Energy Xâ€Ray Detectors for Highly Sensitive Detection and Fastâ€Response Applications. Advanced Materials Technologies, 2021, 6, 2001094.	3.0	23

#	Article	IF	CITATIONS
91	Atomic-layer-deposited ultra-thin VO _x film as a hole transport layer for perovskite solar cells. Semiconductor Science and Technology, 2018, 33, 115016.	1.0	22
92	A General Approach to Probe Dynamic Operation and Carrier Mobility in Fieldâ€Effect Transistors with Nonuniform Accumulation. Advanced Functional Materials, 2019, 29, 1901700.	7.8	22
93	Growth of aligned Cu[sub 2]S nanowire arrays with AAO template and their field-emission properties. Journal of Vacuum Science & Technology an Official Journal of the American Vacuum Society B, Microelectronics Processing and Phenomena, 2004, 22, 1282.	1.6	21
94	Effect of hydrogen treatment on the field emission of amorphous carbon film. Journal of Applied Physics, 2007, 101, 084315.	1.1	21
95	Laser welding of a single tungsten oxide nanotip on a handleable tungsten wire: A demonstration of laser-weld nanoassembly. Applied Physics Letters, 2007, 90, 073103.	1.5	21
96	A study of control growth of three-dimensional nanowire networks of tungsten oxides: From aligned nanowires through hybrid nanostructures to 3D networks. Journal of Crystal Growth, 2010, 312, 520-526.	0.7	21
97	Highly conductive vertically aligned molybdenum nanowalls and their field emission property. Nanoscale Research Letters, 2012, 7, 463.	3.1	21
98	Kilo-Voltage Thin-Film Transistors for Driving Nanowire Field Emitters. IEEE Electron Device Letters, 2020, 41, 405-408.	2.2	21
99	Effect of Contact Mode on the Electrical Transport and Fieldâ€Emission Performance of Individual Boron Nanowires. Advanced Functional Materials, 2010, 20, 1994-2003.	7.8	20
100	Dual-Gate Photosensitive a-Si:H Thin-Film Transistor With a <inline-formula> <tex-math notation="LaTeX">\$pi \$ </tex-math </inline-formula> -Shape Channel for Large-Area Imaging and Sensing. IEEE Electron Device Letters, 2015, 36, 1373-1375.	2.2	20
101	Luminescence properties and site occupancy of Ce ³⁺ in Ba ₂ SiO ₄ : a combined experimental and ab initio study. RSC Advances, 2017, 7, 25685-25693.	1.7	20
102	Fast-response X-ray detector based on nanocrystalline Ga2O3 thin film prepared at room temperature. Applied Surface Science, 2021, 554, 149619.	3.1	20
103	Fully vacuum-sealed addressable nanowire cold cathode flat-panel x-ray source. Applied Physics Letters, 2021, 119, .	1.5	20
104	A moderate synthesis route of 5.6 mA-current LaB ₆ nanowire film with recoverable emission performance towards cold cathode electron source applications. RSC Advances, 2017, 7, 24848-24855.	1.7	19
105	Defect-concentration dependence of electrical transport mechanisms in CuO nanowires. RSC Advances, 2018, 8, 2188-2195.	1.7	19
106	In situ oxygen-assisted field emission treatment for improving the uniformity of carbon nanotube pixel arrays and the underlying mechanism. Carbon, 2011, 49, 3299-3306.	5.4	18
107	Field emission from α-Fe2O3 nanoflakes: Effect of vacuum pressure, gas adsorption and in-situ thermal treatment. Applied Surface Science, 2014, 292, 454-461.	3.1	18
108	Change in crystalline structure of W ₁₈ O ₄₉ nanowires induced by X-ray irradiation and its effects on field emission. RSC Advances, 2018, 8, 752-760.	1.7	18

#	Article	IF	CITATIONS
109	Bayard-Alpert ionization gauge using carbon-nanotube cold cathode. Journal of Vacuum Science & Technology B, 2007, 25, 651.	1.3	17
110	Oscillating current observed in field emission from a single zinc oxide nanostructure and the physical mechanism. Journal of Applied Physics, 2009, 106, .	1.1	17
111	Effects of Pulsewidth and Area of Carbon Nanotube Films on Their Pulsed Field Emission Characteristics. IEEE Transactions on Electron Devices, 2013, 60, 2677-2681.	1.6	17
112	Pulse Field Emission Characteristics of Vertical Few-Layer Graphene Cold Cathode. IEEE Transactions on Electron Devices, 2014, 61, 1771-1775.	1.6	17
113	Self-modulated field electron emitter: Gated device of integrated Si tip-on-nano-channel. Applied Physics Letters, 2016, 109, .	1.5	17
114	<i>In situ</i> sulfur loading in graphene-like nano-cell by template-free method for Li–S batteries. Nanoscale, 2018, 10, 3877-3883.	2.8	17
115	SnO ₂ -rGO nanocomposite as an efficient electron transport layer for stable perovskite solar cells on AZO substrate. Nanotechnology, 2019, 30, 075202.	1.3	17
116	High-Quality All-Inorganic Perovskite CsPbBr ₃ Microsheet Crystals as Low-Loss Subwavelength Exciton–Polariton Waveguides. Nano Letters, 2021, 21, 1822-1830.	4.5	17
117	Noncatastrophic and catastrophic vacuum breakdowns of carbon nanotube film under direct current conditions. Journal of Applied Physics, 2007, 101, 063309.	1.1	16
118	Study of high-brightness flat-panel lighting source using carbon-nanotube cathode. Journal of Vacuum Science & Technology B, 2008, 26, 106.	1.3	16
119	Dual-Gate Photosensitive a-Si:H TFT Array Enabling Fingerprint-Sensor-Integrated Display Application. Journal of Display Technology, 2016, 12, 835-839.	1.3	16
120	Epitaxial growth of multiwall carbon nanotube from stainless steel substrate and effect on electrical conduction and field emission. Nanotechnology, 2017, 28, 305704.	1.3	16
121	High Current Field Emission from Large-Area Indium Doped ZnO Nanowire Field Emitter Arrays for Flat-Panel X-ray Source Application. Nanomaterials, 2021, 11, 240.	1.9	16
122	Polycrystalline Ga ₂ O ₃ Nanostructure-Based Thin Films for Fast-Response Solar-Blind Photodetectors. ACS Applied Nano Materials, 2022, 5, 351-360.	2.4	16
123	Microstructure and property of Czochralski-grown Si–TaSi2 eutectic in situ composite for field emission. Journal of Crystal Growth, 2005, 276, 92-96.	0.7	15
124	Field electron emission of Si nanotips with apexes of various compositions. Applied Physics Letters, 2005, 87, 052105.	1.5	15
125	Controlled synthesis of patterned W18O49 nanowire vertical-arrays and improved field emission performance by in situ plasma treatment. Journal of Materials Chemistry C, 2013, 1, 3217.	2.7	15
126	Design and Realization of Microwave Frequency Multiplier Based on Field Emission From Carbon Nanotubes Cold-Cathode. IEEE Transactions on Electron Devices, 2018, 65, 1146-1150.	1.6	15

#	Article	IF	CITATIONS
127	Fabrication of ZnO Nanowire Field-Emitter Arrays With Focusing Capability. IEEE Transactions on Electron Devices, 2018, 65, 1982-1987.	1.6	15
128	Coplanar-gate ZnO nanowire field emitter arrays with enhanced gate-control performance using a ring-shaped cathode. Scientific Reports, 2018, 8, 12294.	1.6	15
129	Nanostructured High-Performance Thin-Film Transistors and Phototransistors Fabricated by a High-Yield and Versatile Near-Field Nanolithography Strategy. ACS Nano, 2019, 13, 6618-6630.	7.3	15
130	Sensitive and Fast Direct Conversion Xâ€Ray Detectors Based on Singleâ€Crystalline Hgl ₂ Photoconductor and ZnO Nanowire Vacuum Diode. Advanced Materials Technologies, 2020, 5, 1901108.	3.0	15
131	Field-emission fluorescent lamp using carbon nanotubes on a wire-type cold cathode and a reflecting anode. Journal of Vacuum Science & Technology B, 2008, 26, 1700.	1.3	14
132	Intense green-light emission from 9,10-bis (4-(1,2,2-triphenylvinyl)styryl)anthracene emitting electroluminescent devices. Journal of Materials Chemistry C, 2015, 3, 8066-8073.	2.7	14
133	Chemically-doped graphene with improved surface plasmon characteristics: an optical near-field study. Nanoscale, 2016, 8, 16621-16630.	2.8	14
134	Vertically Integrated Optical Sensor With Photoconductive Gain > 10 and Fill Factor > 70%. IEEE Electron Device Letters, 2018, 39, 386-389.	2.2	14
135	Electron emission and structure stability of carbon nanotube cold cathode driven by millisecond pulsed voltage. Vacuum, 2020, 172, 109071.	1.6	14
136	Diagonal 4-in ZnO Nanowire Cold Cathode Flat-Panel X-Ray Source: Preparation and Projection Imaging Properties. IEEE Transactions on Nuclear Science, 2021, 68, 338-345.	1.2	14
137	Study on effect of hydrogen treatment on amorphous carbon film using scanning probe microscopy. Ultramicroscopy, 2009, 109, 451-456.	0.8	13
138	Microstructure change of ZnO nanowire induced by energetic x-ray radiation and its effect on the field emission properties. Nanotechnology, 2013, 24, 275703.	1.3	13
139	Maximum field emission current density of CuO nanowires: theoretical study using a defect-related semiconductor field emission model and in situ measurements. Scientific Reports, 2018, 8, 2131.	1.6	13
140	ZnS nanoparticles coated with graphene-like nano-cell as anode materials for high rate capability lithium-ion batteries. Journal of Materials Science, 2018, 53, 14619-14628.	1.7	13
141	High detectivity ITO/organolead halide perovskite Schottky photodiodes. Semiconductor Science and Technology, 2019, 34, 074004.	1.0	13
142	Realizing the large current field emission characteristics of single vertical few-layer graphene by constructing a lateral graphite heat dissipation interface. Nanoscale, 2021, 13, 5234-5242.	2.8	13
143	Post-treatment of screen-printed carbon nanotube emitter by selective plasma etching. Journal of Vacuum Science & Technology B, 2007, 25, 552.	1.3	12
144	Preparation of Cu ₂ S Dendritic, Double-Comb-Like Nanostructures by Gas-Solid Reaction Method. Journal of Nanoscience and Nanotechnology, 2008, 8, 237-243.	0.9	12

#	Article	IF	CITATIONS
145	Thermal-enhanced field emission from CuO nanowires due to defect-induced localized states. AIP Advances, 2015, 5, 107229.	0.6	12
146	Non-crystallization and enhancement of field emission of cupric oxide nanowires induced by low-energy Ar ion bombardment. Applied Surface Science, 2015, 329, 94-103.	3.1	12
147	Integrated ZnO Nano-Electron-Emitter with Self-Modulated Parasitic Tunneling Field Effect Transistor at the Surface of the p-Si/ZnO Junction. Scientific Reports, 2016, 6, 33983.	1.6	12
148	A two-dimensional structure graphene STM tips fabricated by microwave plasma enhanced chemical vapor deposition. Carbon, 2017, 121, 337-342.	5.4	12
149	One-step growth of graphene-carbon nanotube trees on 4″ substrate and characteristics of single individual tree. Carbon, 2017, 125, 189-198.	5.4	12
150	3-D Dual-Gate Photosensitive Thin-Film Transistor Architectures Based on Amorphous Silicon. IEEE Transactions on Electron Devices, 2017, 64, 4952-4958.	1.6	12
151	Defective WO _{3â^'x} nanowire: possible long lifetime semiconductor nanowire point electron source. Nanoscale, 2019, 11, 3370-3377.	2.8	12
152	Pyramid-Shaped Single-Crystalline Nanostructure of Molybdenum with Excellent Mechanical, Electrical, and Optical Properties. ACS Applied Materials & Interfaces, 2020, 12, 24218-24230.	4.0	12
153	How Materials and Device Factors Determine the Performance: A Unified Solution for Transistors with Nontrivial Gates and Transistor–Diode Hybrid Integration. Advanced Science, 2022, 9, e2104896.	5.6	12
154	Fabrication and field emission properties of boron nanowire bundles. Ultramicroscopy, 2009, 109, 447-450.	0.8	11
155	Pulsed-laser treatment of solution-grown ZnO nanowires in nitrogen: Enhancing in electrical conduction and field emission. Journal of Applied Physics, 2010, 107, 024312.	1.1	11
156	Effects of X-ray irradiation on the structure and field electron emission properties of vertically aligned few-layer graphene. Nuclear Instruments & Methods in Physics Research B, 2013, 304, 49-56.	0.6	11
157	Origin of the ring-shaped emission pattern observed from the field emission of ZnO nanowire: role of adsorbates and electron initial velocity. Materials Research Express, 2014, 1, 045050.	0.8	11
158	A simple SVS method for obtaining large-scale WO ₃ nanowire cold cathode emitters at atmospheric pressure and low temperature. CrystEngComm, 2015, 17, 1065-1072.	1.3	11
159	Molybdenum Nanoscrews: A Novel Non-coinage-Metal Substrate for Surface-Enhanced Raman Scattering. Nano-Micro Letters, 2017, 9, 2.	14.4	11
160	Highly stable field emission from ZnO nanowire field emitters controlled by an amorphous indium–gallium–zinc-oxide thin film transistor. Japanese Journal of Applied Physics, 2018, 57, 045003.	0.8	11
161	A Plasmon-Mediated Electron Emission Process. ACS Nano, 2019, 13, 1977-1989.	7.3	11
162	Fabrication of Coaxis-Gated ZnO Nanowire Field-Emitter Arrays With In-Plane Focusing Gate Electrode Structure. IEEE Transactions on Electron Devices, 2020, 67, 677-683.	1.6	11

#	Article	IF	CITATIONS
163	Pixellated Perovskite Photodiode on IGZO Thin Film Transistor Backplane for Low Dose Indirect X-Ray Detection. IEEE Journal of the Electron Devices Society, 2021, 9, 96-101.	1.2	11
164	Microfabrication and characterization of an array of diode electron source using amorphous diamond thin films. Applied Physics Letters, 2000, 77, 2921-2923.	1.5	10
165	A cold cathode lighting element prototype. Ultramicroscopy, 2003, 95, 81-84.	0.8	10
166	Fabrication and field emission performance of arrays of vacuum microdiodes containing CuO nanowire emitters grown directly on glass without a catalyst. Science Bulletin, 2011, 56, 906-911.	1.7	10
167	Phonon-assisted field emission from W18O49 nanowires. Applied Physics Letters, 2013, 103, 141915.	1.5	10
168	A Numerical Study of an Amorphous Silicon Dual-Gate Photo Thin-Film Transistor for Low-Dose X-Ray Imaging. Journal of Display Technology, 2015, 11, 646-651.	1.3	10
169	Penetration length-dependent hot electrons in the field emission from ZnO nanowires. Applied Surface Science, 2018, 427, 573-580.	3.1	10
170	Investigation of the temperature dependent field emission from individual ZnO nanowires for evidence of field-induced hot electrons emission. Journal of Physics Condensed Matter, 2018, 30, 315002.	0.7	10
171	The Growth Methods and Field Emission Studies of Low-Dimensional Boron-Based Nanostructures. Applied Sciences (Switzerland), 2019, 9, 1019.	1.3	10
172	Stable Heating Above 900 K in the Field Emission of ZnO Nanowires: Mechanism for Achieving High Current in Large Scale Field Emitter Arrays. Advanced Electronic Materials, 2020, 6, 2000624.	2.6	10
173	Terahertz laser diode using field emitter arrays. Physical Review B, 2021, 103, .	1.1	10
174	A Study of Field Electron Emission from Thin Amorphous-Carbon-Nitride Films. Chinese Physics Letters, 1998, 15, 539-541.	1.3	9
175	Study of field electron emission from nanocrystalline diamond thin films grown from a N2/CH4microwave plasma. Journal Physics D: Applied Physics, 2000, 33, 1572-1575.	1.3	9
176	Experimental evidence of resonant field emission from ultrathin amorphous diamond thin film. Surface and Interface Analysis, 2004, 36, 461-464.	0.8	9
177	Effect of surface treatment on printed carbon nanotube field emitters. Surface and Interface Analysis, 2004, 36, 485-488.	0.8	9
178	Field emission properties from aligned carbon nanotube films with tetrahedral amorphous carbon coatings. Diamond and Related Materials, 2006, 15, 1462-1466.	1.8	9
179	Arrays of vacuum microdiodes using uniform diamondlike-carbon tip apexes. Applied Physics Letters, 2006, 89, 233518.	1.5	9
180	Three-dimensional six-fold symmetry ZnO sub-microstructures. Journal of Crystal Growth, 2009, 311, 1435-1440.	0.7	9

#	Article	IF	CITATIONS
181	Tunable field emission characteristics of ZnO nanowires coated with varied thickness of lanthanum boride thin films. Ultramicroscopy, 2013, 132, 36-40.	0.8	9
182	Effect of Nanostructure Building Formation on High Current Field Emission Properties in Individual Molybdenum Nanocones. ACS Applied Materials & Interfaces, 2015, 7, 3825-3833.	4.0	9
183	Highly Photosensitive Dual-Gate a-Si:H TFT and Array for Low-Dose Flat-Panel X-Ray Imaging. IEEE Photonics Technology Letters, 2016, 28, 1952-1955.	1.3	9
184	Effect of Piezoresistive Behavior on Electron Emission from Individual Silicon Carbide Nanowire. Nanomaterials, 2019, 9, 981.	1.9	9
185	Highly Stable Field Emission from a Tungsten Diselenide Monolayer on Zinc Oxide Nanowire by Geometrically Modulating Hot Electrons. Advanced Electronic Materials, 2019, 5, 1900128.	2.6	9
186	DP3 signal as a neuro-indictor for attentional processing of stereoscopic contents in varied depths within the †̃comfort zone'. Displays, 2020, 63, 101953.	2.0	9
187	Highly-Sensitive Indirect-Conversion X-Ray Detector With an Embedded Photodiode Formed by a Three-Dimensional Dual-Gate Thin-Film Transistor. Journal of Lightwave Technology, 2020, 38, 3775-3780.	2.7	9
188	Pulsed voltage driving enhanced electron emission in ZnO nanowire cold cathode flat-panel X-ray source. Vacuum, 2022, 199, 110970.	1.6	9
189	The intrinsic relation between field electron emission and structure characteristics of amorphous diamond film. Journal Physics D: Applied Physics, 2000, 33, 2568-2572.	1.3	8
190	Synthesis of silicon carbide nano-junctions in a catalyst-assisted process. Chemical Physics Letters, 2002, 364, 608-611.	1.2	8
191	Preparation and characterization of nanostructured film of graphitized diamond crystallites for field electron emission. Journal of Applied Physics, 2003, 94, 5429.	1.1	8
192	Improving field-emission uniformity of large-area W[sub 18]O[sub 49] nanowire films by electrical treatment. Journal of Vacuum Science & Technology B, 2009, 27, 2420.	1.3	8
193	Anomalous temperature dependence of field emission from W18O49 nanowires caused by surface states and field penetration. Journal of Applied Physics, 2014, 116, 133506.	1.1	8
194	Quasi-Saturated Arsenic Concentration and Uniform Electron Emission by Regulating Thermal Oxidation of Si Nanotips. IEEE Transactions on Electron Devices, 2019, 66, 1545-1551.	1.6	8
195	Ultrafast Electron Tunneling Devices—From Electricâ€Field Driven to Opticalâ€Field Driven. Advanced Materials, 2021, 33, e2101449.	11.1	8
196	Sensitive direct-conversion X-ray detectors formed by ZnO nanowire field emitters and β-Ga ₂ O ₃ photoconductor targets with an electron bombardment induced photoconductivity mechanism. Photonics Research, 2021, 9, 2420.	3.4	8
197	Characterization of a high voltage flat panel display unit using nanotube-based emitters. Ultramicroscopy, 2001, 89, 105-109.	0.8	7
198	Analysis of the field-electron energy distribution from amorphous carbon-nitride films. Journal of Vacuum Science & Technology an Official Journal of the American Vacuum Society B, Microelectronics Processing and Phenomena, 2003, 21, 567.	1.6	7

#	Article	IF	CITATIONS
199	Achieving uniform field emission from carbon nanotube composite cold cathode with different carbon nanotube contents: Effects of conductance and plasma treatment. Ultramicroscopy, 2009, 109, 390-394.	0.8	7
200	In Situ Characterization of the Local Work Function along Individual Free Standing Nanowire by Electrostatic Deflection. Scientific Reports, 2016, 6, 21270.	1.6	7
201	An Analytical Modeling of Field Electron Emission for a Vertical Wedged Ordered Nanostructure. Advanced Electronic Materials, 2017, 3, 1700295.	2.6	7
202	Band-to-Band Tunneling-Dominated Thermo-Enhanced Field Electron Emission from p-Si/ZnO Nanoemitters. ACS Applied Materials & Interfaces, 2018, 10, 21518-21526.	4.0	7
203	Structure stability of few-layer graphene under high electric field. Carbon, 2019, 144, 202-205.	5.4	7
204	Flexible indirect x-ray detector enabled by organic photodiode and CsPbBr ₃ perovskite quantum dot scintillator. Flexible and Printed Electronics, 2021, 6, 015008.	1.5	7
205	Abnormal Electron Emission in a Vertical Graphene/Hexagonal Boron Nitride van der Waals Heterostructure Driven by a Hot Hole-Induced Auger Process. ACS Applied Materials & Interfaces, 2020, 12, 57505-57513.	4.0	7
206	Effects of the surface treatment of silicon substrate on the field emission characteristic of a silicon and amorphous diamond cold cathode emitter. Ultramicroscopy, 1999, 79, 89-93.	0.8	6
207	Substrate nanoprotrusions and their effect on field electron emission from amorphous-diamond films. Applied Physics Letters, 2002, 80, 4030-4032.	1.5	6
208	Field electron emission properties from aligned carbon nanotube bundles of different density. Surface and Interface Analysis, 2004, 36, 501-505.	0.8	6
209	Damages of screen-printed carbon nanotube cold cathode during the field emission process. Ultramicroscopy, 2009, 109, 385-389.	0.8	6
210	Field emission properties of α-Fe2O3 nanotips prepared on indium tin oxide coated glass by thermal oxidation of iron film. Journal of Vacuum Science and Technology B:Nanotechnology and Microelectronics, 2010, 28, C2B34-C2B37.	0.6	6
211	Low-temperature Synthesis of Large-area Films of Molybdenum Trioxide Microbelts in Air and the Dependence of Their Field Emission Performance on Growth Conditions. Journal of Materials Science and Technology, 2010, 26, 584-588.	5.6	6
212	<i>In situ</i> study of graphene crystallinity effect on field electron emission characteristics. Journal of Vacuum Science and Technology B:Nanotechnology and Microelectronics, 2017, 35, .	0.6	6
213	Fast identification of the conduction-type of nanomaterials by field emission technique. Scientific Reports, 2017, 7, 13057.	1.6	6
214	An easy way to controllably synthesize one-dimensional SmB 6 topological insulator nanostructures and exploration of their field emission applications. Chinese Physics B, 2017, 26, 118103.	0.7	6
215	Tungsten Target Optimization for Photon Fluence Maximization of a Transmission-Type Flat-Panel X-Ray Source by Monte Carlo Simulation and Experimental Measurement. IEEE Transactions on Radiation and Plasma Medical Sciences, 2018, 2, 452-458.	2.7	6
216	Energy-tunable photon-enhanced thermal tunneling electrons for intrinsic adaptive full spectrum solar energy conversion. Applied Physics Letters, 2020, 116, .	1.5	6

#	Article	IF	CITATIONS
217	Lowâ€Temperature Fabrication of Cold Cathode WO ₂ Nanowire Arrays on Glass Substrate and Improvement of their Working Performance. Advanced Materials Technologies, 2017, 2, 1700029.	3.0	6
218	Fully Vacuum-Sealed Diode-Structure Addressable ZnO Nanowire Cold Cathode Flat-Panel X-ray Source: Fabrication and Imaging Application. Nanomaterials, 2021, 11, 3115.	1.9	6
219	Effects of the interface and surface nanostructures on field emission of amorphous diamond film. Journal of Vacuum Science & Technology an Official Journal of the American Vacuum Society B, Microelectronics Processing and Phenomena, 2003, 21, 581.	1.6	5
220	Fine-structured field emission images originating from coherently scattering of electrons within a multi-walled carbon nanotube. Applied Surface Science, 2007, 254, 1389-1393.	3.1	5
221	Self-Assembly of Au-Ag Alloy Nanoparticles by Thermal Annealing. Journal of Nanoscience and Nanotechnology, 2008, 8, 3487-3492.	0.9	5
222	Preparation and field emission property of nanodiamond-cluster-embedded diamondlike carbon film. Journal of Vacuum Science & Technology B, 2008, 26, 1321.	1.3	5
223	Field emission characteristics of screen-printed carbon nanotubes cold cathode by hydrogen plasma treatment. Applied Surface Science, 2011, 258, 738-742.	3.1	5
224	Correlation between surface chemistry, gasochromism and field emission properties of tungsten oxide nanowire thin films when exposed to atomic oxygen. RSC Advances, 2015, 5, 70059-70063.	1.7	5
225	Electrical properties of fluorine-doped ZnO nanowires formed by biased plasma treatment. Physica E: Low-Dimensional Systems and Nanostructures, 2018, 99, 254-260.	1.3	5
226	Pinhole evolution of few-layer graphene during electron tunneling and electron transport. Carbon, 2018, 139, 688-694.	5.4	5
227	39â€2: Highly Sensitive a‧i:H PIN Photodiode Gated LTPS TFT for Optical Inâ€Display Fingerprint Identification. Digest of Technical Papers SID International Symposium, 2018, 49, 490-493.	0.1	5
228	Si Nanowire With Integrated Space-Charge- Limited Conducted Schottky Junction for Enhancing Field Electron Emission and Its Gated Devices. IEEE Transactions on Electron Devices, 2020, 67, 4467-4472.	1.6	5
229	Theoretical Analysis and Verification of Electron-Bombardment-Induced Photoconductivity in Vacuum Flat-Panel ÂDetectors. Journal of Lightwave Technology, 2021, 39, 2618-2624.	2.7	5
230	Recent Progress on ZnO Nanowires Cold Cathode and Its Applications. Nanomaterials, 2021, 11, 2150.	1.9	5
231	Study of the Interface Interaction Mechanism Between 9,10-Bis(4-(1,2,2-triphenylvinyl)) Tj ETQq1 1 0.784314	rgBT/Overl	ock ₅ 10 Tf 50
232	Study of the frequency response of the thin film cold cathode electron source of a lighting element. Ultramicroscopy, 2001, 89, 123-128.	0.8	4
233	Study of techniques for improving emission uniformity of gated CuO nanowire field emitter arrays. Journal of Vacuum Science and Technology B:Nanotechnology and Microelectronics, 2010, 28, C2C45-C2C48.	0.6	4
234	Improvement of field emission properties of α-Fe2O3 nanoflakes due to the lowered back contact barrier after high energy X-ray irradiation. Journal of Applied Physics, 2013, 114, .	1.1	4

#	Article	lF	CITATIONS
235	The Effect of <italic>In situ</italic> Magnetic Field on Magnetic Properties and Residual Stress of Fe-Based Amorphous Film. IEEE Transactions on Magnetics, 2018, 54, 1-8.	1.2	4
236	Tetragonal Singleâ€Crystalline Boron Nanowires with Strong Anisotropic Light Scattering Behaviors and Photocurrent Response in Visibleâ€Light Regime. Small, 2018, 14, e1704135.	5.2	4
237	Mechanism of photoluminescence quenching in visible and ultraviolet emissions of ZnO nanowires decorated with gold nanoparticles. Japanese Journal of Applied Physics, 2019, 58, 051005.	0.8	4
238	Photovoltage-Coupled Dual-Gate InGaZnO Thin-Film Transistors Operated at the Subthreshold Region for Low-Power Photodetection. ACS Applied Electronic Materials, 2020, 2, 1745-1751.	2.0	4
239	Vertical Transistors with Conductive-Network Electrodes: A Physical Image and What It Tells. Physical Review Applied, 2020, 13, .	1.5	4
240	Self-Optimizing Effect of a Few-Layer Graphene's Top-Edge Structure during Field Electron Emission Observed by In Situ TEM. ACS Applied Materials & Interfaces, 2020, 12, 16815-16821.	4.0	4
241	Concept for Realizing High Output Power Density Thermionic Energy Convertor by Field-Assisted Thermionic Emission Using a Direct-Tunneling Metal–Insulator–Graphene Cathode. IEEE Transactions on Electron Devices, 2021, 68, 4144-4149.	1.6	4
242	Preparation, structure configuration, physical properties and applications of borophene and two-dimensional alkaline-earth metal boride nanomaterials. Wuli Xuebao/Acta Physica Sinica, 2017, 66, 217702.	0.2	4
243	Gated Si-Tip With On-Tip Integrated Gate-All-Around Field Effect Transistor for Actively Controlled Field Electron Emission. IEEE Electron Device Letters, 2022, 43, 466-469.	2.2	4
244	Microfabrication and characterization of gated amorphous diamond-based field emission electron sources. Ultramicroscopy, 2001, 89, 111-118.	0.8	3
245	Resonant field emission through amorphous diamond thin films (a model study). Ultramicroscopy, 2003, 95, 75-80.	0.8	3
246	The Frequency Characteristics of a Lighting Element Using Carbon Nanotube-Based Composite Cold-Cathode. IEEE Transactions on Electron Devices, 2005, 52, 1504-1507.	1.6	3
247	The influence of temperature and electric field on field emission energy distribution of an individual single-wall carbon nanotube. Applied Physics Letters, 2009, 94, 263105.	1.5	3
248	Improved Field Emission Characteristics of Large-Area Films of Molybdenum Trioxide Microbelt. Journal of Nanomaterials, 2010, 2010, 1-6.	1.5	3
249	Double-gate-driving field emission display panel with stacked-metalized-aperture structure. Journal of Vacuum Science and Technology B:Nanotechnology and Microelectronics, 2010, 28, C2D15-C2D21.	0.6	3
250	The effect of amorphous carbon layer on the field emission characteristics of carbon nanotube film. Ultramicroscopy, 2011, 111, 426-430.	0.8	3
251	Molybdenum Nanowall Cold Cathode With High Resistance to Oxidizing Environment. IEEE Transactions on Electron Devices, 2014, 61, 1760-1763.	1.6	3
252	Dual-gate photo thin-film transistor: a "smart―pixel for high- resolution and low-dose X-ray imaging. Journal of Physics: Conference Series, 2015, 619, 012023.	0.3	3

#	Article	IF	CITATIONS
253	Three-dimensional fin-shaped dual-gate photosenstive a-Si:H thin-film transistor for low dose X-ray imaging. , 2016, , .		3
254	Introduction to the micro/nano-fabrication of modern vacuum electronic devices. , 2017, , .		3
255	Improved field emission properties of <i>α</i> -Fe ₂ O ₃ nanoflakes with current aging treatment and morphology optimization. Nanotechnology, 2018, 29, 085708.	1.3	3
256	An in situ characterization technique for electron emission behavior under a photo-electric-common-excitation field: study on the vertical few-layer graphene individuals. Nanotechnology, 2019, 30, 445202.	1.3	3
257	Non-uniaxial stress-assisted fabrication of nanoconstriction on vertical nanostructured Si. Nanotechnology, 2019, 30, 365601.	1.3	3
258	3D Spherical Panoramic Epipolar Line Based on Essential Matrix. IEEE Access, 2020, 8, 192165-192176.	2.6	3
259	Backside Illuminated 3-D Photosensitive Thin-Film Transistor on a Scintillating Glass Substrate for Indirect-Conversion X-Ray Detection. IEEE Electron Device Letters, 2020, 41, 1209-1212.	2.2	3
260	A Universal Method to Weld Individual One-Dimensional Nanostructures with a Tungsten Needle Based on Synergy of the Electron Beam and Electrical Current. Nanomaterials, 2020, 10, 469.	1.9	3
261	Study on Pyramidal Molybdenum Nanostructures Cold Cathode with Large-Current Properties Based on Self-Assembly Growth Method. ACS Applied Materials & Interfaces, 2020, 12, 35354-35364.	4.0	3
262	High-performance x-ray source based on graphene oxide-coated Cu2S nanowires grown on copper film. Nanotechnology, 2020, 31, 485202.	1.3	3
263	Self-Assembly of Au-Ag Alloy Nanoparticles by Thermal Annealing. Journal of Nanoscience and Nanotechnology, 2008, 8, 3487-3492.	0.9	3
264	Achieving High Current Stability of Gated Carbon Nanotube Cold Cathode Electron Source Using IGBT Modulation for X-ray Source Application. Nanomaterials, 2022, 12, 1882.	1.9	3
265	Fabrication and characterization of a field emission display prototype for indoor giant display application. Journal of Vacuum Science & Technology B, 2007, 25, 1569.	1.3	2
266	Microstructure and properties of Si-TaSi2 eutectic in situ composite for field emission. Science Bulletin, 2007, 52, 984-989.	1.7	2
267	In-situ determination of the flat band carrier concentration and surface charge density of individual semiconductor nanowires by a combination of electrical and field emission measurements. Journal of Applied Physics, 2017, 121, 174306.	1.1	2
268	Fabrication of ZnO nanowire field emitter arrays with non-coplanar focus electrode structure. , 2017, , .		2
269	Fabrication of large-area arrays of coaxial gated ZnO nanowire field emitters for vacuum microelectronics applications. , 2017, , .		2
270	Field emission characteristics of individual ZnO nanowire before vacuum breakdown. , 2018, , .		2

#	Article	IF	CITATIONS
271	Cathodoluminescent Properties of polycrystalline Ga ₂ O ₃ thin film and its application UV flat panel light source. , 2020, , .		2
272	Addressable field emitter arrays with high density patterned ZnO nanowire emitters and under-gate structure. , 2020, , .		2
273	Performance Enhancement of Terahertz Laser Diode via Resonant Cavities. IEEE Transactions on Electron Devices, 2021, 68, 6465-6469.	1.6	2
274	Widely Adjusting the Breakdown Voltages of Kilo-Voltage Thin Film Transistors. IEEE Electron Device Letters, 2022, 43, 240-243.	2.2	2
275	Drain Current Drop in Oxide Semiconductor Thin-Film Transistors: The Mechanisms and a Solution. IEEE Transactions on Electron Devices, 2022, 69, 2430-2435.	1.6	2
276	Template-based synthesis of carbon nanofibres and their field emission characteristics. Surface and Interface Analysis, 2004, 36, 493-496.	0.8	1
277	Patterned growth and field emission properties of ZnO nanowires prepared by thermal oxidation method. , 2010, , .		1
278	Evaluation of a simplified simulation approach for thin film type gated field emitters. Journal of Vacuum Science and Technology B:Nanotechnology and Microelectronics, 2011, 29, 02B102.	0.6	1
279	Growth of a single graphene sheet on a tungsten tip. , 2014, , .		1
280	In-situ measurement of temperature dependence of emission current and pressure of a fully-sealed ZnO nanowire field emission device. , 2014, , .		1
281	ZnO nanowire field electron emitters. , 2015, , .		1
282	Field emission properties of boron nanostructures. , 2015, , .		1
283	Comparative study of field emission from individual ZnO nanowire with and without NH <inf>3</inf> plasma treatment. , 2015, , .		1
284	Modulation of field emission current from ZnO nanowires by high voltage a-Si thin film transistor. , 2015, , .		1
285	Fabrication of ZnO nanowire field emitter arrays with self-aligned focus electrode structure. , 2016, ,		1
286	Fabrication of single crystalline SmB <inf>6</inf> nanocone arrays and investigation of their field emission properties. , 2016, , .		1
287	Si tip with integrated nano-channel: Self-heated and self-current-limited field electron emitter. , 2017, ,		1
288	ZnO nanowire field emitters integrated with amorphous Indium-Gallium-Zinc-Oxide thin film		1

transistor., 2017,,.

#	Article	IF	CITATIONS
289	A Direct-Conversion X-ray Detector Based on A Vertical X-ray Photoconductor-Gated a-IGZO TFT. , 2018, , .		1
290	An 8-inch diagonal ZnO nanowire cold cathode panel for flat-panel X-ray source. , 2018, , .		1
291	In situ study of field emission vacuum breakdown of individual multiâ€wall carbon nanotube. Micro and Nano Letters, 2019, 14, 206-210.	0.6	1
292	Optimization of PMMA:PCBM Interlayer for MAPbI ₃ /IGZO Phototransistor. , 2020, , .		1
293	Theoretical analysis of efficiency for vacuum photoelectric energy converters with plasmon-enhanced electron emitter. Journal of Applied Physics, 2021, 130, 023104.	1.1	1
294	Highly Sensitive Directâ€Conversion Vacuum Flatâ€Panel Xâ€Ray Detectors Formed by Ga 2 O 3 â€ZnO Heterojunction Cold Cathode and ZnS Target and their Photoelectron Multiplication Mechanism. Advanced Materials Interfaces, 0, , 2102268.	1.9	1
295	A Microelectronic Terahertz Source Using Multiple Field Emitter Cathodes With an Array of Coupled Cavities. IEEE Transactions on Electron Devices, 2022, 69, 2618-2624.	1.6	1
296	Optimizing Performance of Coaxis Planar-Gated ZnO Nanowire Field-Emitter Arrays by Tuning Pixel Density. Nanomaterials, 2022, 12, 870.	1.9	1
297	Influence of the optimal etching conditions of silicon substrates on field-electron emission from amorphous-diamond films. Journal of Vacuum Science & Technology an Official Journal of the American Vacuum Society B, Microelectronics Processing and Phenomena, 2003, 21, 618.	1.6	0
298	Acid treatment of carbon nanofibres with encapsulated catalytic iron nanoparticles. Surface and Interface Analysis, 2004, 36, 497-500.	0.8	0
299	Field Emission Characteristics of ZnO Nanowire and Its Application to Luminescent Tubes. , 2006, , .		Ο
300	Post Treatment of Screen-Printed Carbon Nanotubes Emitter by Plasma Etching. , 2006, , .		0
301	Controlling growth of aligned carbon nanotube bundles arrays with microwave plasma CVD. , 2006, , .		0
302	Field emission characteristics of polymethyl methacrylate polymer thin film. Journal of Vacuum Science & Technology B, 2007, 25, 604.	1.3	0
303	Field emission from vertically aligned silicon nanotubes. , 2007, , .		0
304	Low temperature growth of carbon nanotube on glass substrate and its application in field emission display. , 2007, , .		0
305	Fabrication of ultra-sharp ZnO nanotip from sub-micro ZnO whiskers by electric field treatment. , 2007, , .		Ο
306	Study of large-area vacuum microelectronic arrays using nanoemitters and their application in field emission flat panel display. , 2009, , .		0

#	Article	IF	CITATIONS
307	Synthesis and field emission properties of large-area arrays of tungsten oxide pencil-like nanostructure. , 2009, , .		0
308	An industrial method for low-temperature synthesis of large-area films of molybdenum trioxide microbelts and their field emission property. , 2009, , .		0
309	No-catalyst growth of vertically-aligned AlN nanocone field electron emitter arrays with high emission performance at low temperature. Chinese Physics B, 2010, 19, 107205.	0.7	0
310	P2–19: A scheme of uniformity measuring for flat plane cold cathode. , 2010, , .		0
311	Fabrication of patterned aligned W <inf>18</inf> O <inf>49</inf> nanowire arrays with high field emission performances. , 2010, , .		0
312	P2–16: Field emission properties of α-Fe <inf>2</inf> 0 <inf>3</inf> nanostructures prepared from iron thin film with different thickness. , 2010, , .		0
313	P1–3: Optimization of structure parameters of gated nanowire field emitters for field emission display application. , 2010, , .		0
314	A polycrystalline metallic molybdenum nanotips: Synthesis, electrical conductivity and field emission properties. , 2012, , .		0
315	Field emission from copper micro-cones formed by ion bombardment of copper substrate using an oxide masking. , 2012, , .		0
316	Optimization of insulator layer with high breakdown voltage for 10 inch nanowire field emission display. , 2012, , .		0
317	Study of the working performance of WO <inf>2</inf> nanowire arrays in gated field emission display devices. , 2012, , .		0
318	Simulation of effects of geometrical parameters on the performance of a gated CuO nanowire cold cathode vacuum triode. , 2012, , .		0
319	Temperature dependence of the field-emission from the tungsten oxide nanowires. , 2012, , .		0
320	Field emission characteristics of graphene film on nickel substrate. , 2012, , .		0
321	The Controlled Growth of Long AlN Nanorods and In-situ Investigation on Their Field Emission Properties. , 0, , .		0
322	Direct synthesis of carbon nanotube on stainless steel cathode. , 2013, , .		0
323	10 inch screen printed ZnO nanowire cold cathode for flat panel light source. , 2013, , .		0
324	Synthesis of WO <inf>2</inf> nanowire arrays on glass substrate for field emission application. , 2013,		0

#	Article	IF	CITATIONS
325	Non-crystallization and enhancement of field emission of cupric oxide nanowires induced by low-energy Ar Ion bombardment. , 2013, , .		0
326	In situ oxidizing environment field emission study of Mo nanowall cold cathode. , 2014, , .		0
327	A self-aligned approach to fabricate planar gated nanowires field emitter arrays. , 2014, , .		Ο
328	Defect-assisted field emission from ZnO nanotrees. , 2014, , .		0
329	Precise evaluation of LCD gray-to-gray response time based on a reference pattern synchronous measurement using high speed charge-coupled device camera. Journal of the Society for Information Display, 2014, 22, 429-436.	0.8	0
330	Evaluation of a single-pixel one-transistor active pixel sensor for fingerprint imaging. , 2015, , .		0
331	Evaluation of a single-pixel one-transistor active pixel sensor for low-dose indirect-conversion X-ray imaging. , 2015, , .		0
332	Exploring the Intrinsic Piezofluorochromic Mechanism of TPE-An by STS Technique. Nanoscale Research Letters, 2015, 10, 1036.	3.1	0
333	Design, optimization and evaluation of a "smart―pixel sensor array for low-dose digital radiography. Proceedings of SPIE, 2016, , .	0.8	Ο
334	Effect of crystallinity of graphene on its field emission character. , 2016, , .		0
335	Tuning field emission properties of tungsten trioxide nanowires for flat panel X-ray source application. , 2016, , .		0
336	Field emission behaviors of B/LaB <inf>6</inf> hierarchical heterojunction nanostructures. , 2016, , .		0
337	Design methodology for a fingerprint sensor-integrated display pixel and array based on dual-gate a-Si:H photosensitive TFT. , 2016, , .		0
338	A fluorescence detector for rapid on-chip detection of amniotic fluid embolism biomarker based on dual-gate photosensitive thin-film transistor. , 2016, , .		0
339	Molybdenum nano emitters: the effect of the structural feature on oxygen damage immunity. Materials Research Express, 2016, 3, 045001.	0.8	0
340	Fabrication of amorphous IGZO thin film transistor for active-driving of ZnO nanowire field emitters. , 2016, , .		0
341	Fabrication of transparent gated ZnO nanowire field emitter arrays. , 2016, , .		0
342	A case for ZnO nanowire field emitter arrays in advanced x-ray source applications. , 2016, , .		0

#	Article	IF	CITATIONS
343	Field emission characteristics of carbon nanotube cold cathode by driving millisecond width pulse voltage. , 2016, , .		0
344	Single crystalline metallic molybdenum nano-pyramids: Preparation and high current field emission properties. , 2016, , .		0
345	In-situ study of surface work function, electrical characteristic and field emission property of individual ZnO nanowire. , 2016, , .		0
346	Fabrication and characterization of gated ZnO nanowire field electron emitters. , 2016, , .		0
347	Optimization of metal anode layer for transmission anode flat panel X-ray source using ZnO nanowire FEAs. , 2017, , .		0
348	The experimental characterization of vacuum breakdown in pulsed field emission from individual carbon nanotube. , 2017, , .		0
349	Preparation of ZnO nanowires for high emission current field emitter arrays. , 2017, , .		0
350	Preparation of ZnO nanowires for a transparent cold cathode panel and its application in light source. , 2017, , .		0
351	Light-responsive field emission for display applications. , 2017, , .		0
352	Evolution of field emission pattern of few-layer graphene with different edge morphology. , 2017, , .		0
353	Capture field emission pattern image of carbon nanotubes by using electron beam scanning analyzer. , 2017, , .		0
354	Effect of the electrical properties on the field emission properties of CuO nanowires. , 2017, , .		0
355	Double-sided masking and stress-release etching for the fabrication of high-aspect-ratio graphene micro-cantilever. Journal of Micromechanics and Microengineering, 2018, 28, 085001.	1.5	0
356	Effect of Pressure on Field Emission Pattern from ZnO Nanowires. , 2018, , .		0
357	Field Emission Properties of Indium-Doped ZnO Nanowires Prepared on ITO Glass Substrate. , 2018, , .		0
358	Interface Control for Enhancing Field Emission Properties from Single-Crystalline Molybdenum Nanopyramid Emitters. , 2018, , .		0
359	Field emission from Au nanoparticles decorated ZnO nanowires. , 2018, , .		Ο
360	Controlled Preparation of Micron-Size-Pattemed ZnO Nanowire Field Emitters. , 2018, , .		0

#	Article	IF	CITATIONS
361	Field Emission Properties of a Single Silicon Carbide Nanowire. , 2018, , .		Ο
362	Field Emission from Oxide Nanowires: Mechanism and Applications. , 2018, , .		0
363	Thermo-enhanced field electron emission by bandto-ban tunneling from p-Si/ZnO nano-emitters. , 2018, , .		Ο
364	Si-Tips with Saturated High Concentration Arsenic Dopant at the Nano-Apexes for Uniform Field Electron Emission. , 2018, , .		0
365	Mechanism of non-saturated field electron emission from gated p-type Si tips. , 2018, , .		Ο
366	In-situ Characterization of Structure Evolution of Graphene During Field Emission. , 2018, , .		0
367	Defect-enhanced field electron emission from WO3â^'x nanowires. , 2019, , .		Ο
368	The photoresponse of ZnO nanowire cold cathode flat panel detector using ZnS photoconductor. , 2019, , .		0
369	Fabrication of Gated ZnO Nanowire Field Emitter Arrays for Pulsed Flat Panel X-ray Source. , 2020, , .		Ο
370	Space-Charge-Limited Conduction in Forward Biased Schottky Junction and Its Effect on Field Emission from Crystalline Gold-Silver Alloy Nanoparticle Decorated Si Nanowire. , 2020, , .		0
371	Fabrication of ZnO nanowire cold cathode flat panel X-ray source module for adaptive X-ray imaging. , 2020, , .		Ο
372	Pâ€1.6: Characteristics of High Voltage Corbino aâ€IGZO Thinâ€film Transistor. Digest of Technical Papers SID International Symposium, 2021, 52, 695-695.	0.1	0
373	Pâ€1.8: A 3â€Probe Approach to Study Dynamic Operation in High Voltage Thin Film Transistors. Digest of Technical Papers SID International Symposium, 2021, 52, 699-699.	0.1	0
374	WO3 nanowire field emission point electron source with high brightness and current stability. Vacuum, 2021, , 110660.	1.6	0
375	ZnO Nanowire Field Emitter Arrays: Fabrication, Field Emission Mechanism and Applications. , 2015, , .		0
376	A Microfluidic Fluorescence Biosensor Based on Three-Dimensional Dual-Gate Photosensitive Thin-Film Transistor. , 2017, , .		0
377	Development of gated carbon nanotube cold cathode for miniature X-ray source. , 2021, , .		0
378	Optimization of Gated ZnO Nanowire Field-Emitter Arrays by Tuning Pixel Density. , 2021, , .		0

#	Article	IF	CITATIONS
379	Cold Cathode X-Ray Flat Panel Detector Based on Ga2O3 Thin Film Photoconductor. , 2021, , .		0
380	Fabrication of ZnO nanowires cold cathode X-ray source with micro patterned transmission anode. , 2021, , .		0
381	Field Emission Characteristics of ZnO Nanowire Driven by Pulsed Voltage. , 2021, , .		0
382	Pixelated Vacuum Flat Panel Detector Using ZnS Photoconductor and ZnO Nanowires Cold Cathode. Nanomaterials, 2022, 12, 884.	1.9	0
383	P-Type Si-Tips With Integrated Nanochannels for Stable Nonsaturated High Current Density Field Electron Emission. IEEE Transactions on Electron Devices, 2022, 69, 3908-3913.	1.6	0
384	Quantitative Analysis on the Field Strength in the Addressable Gated ZnO Nanowire Field Emitter Arrays: Model and Experiment. IEEE Transactions on Electron Devices, 2022, 69, 5206-5210.	1.6	0